



Tunable phononic crystals based on cylindrical Hertzian contact

Feng Li, Duc Ngo, Jinkyu Yang, and Chiara Daraio

Citation: [Applied Physics Letters](#) **101**, 171903 (2012); doi: 10.1063/1.4762832

View online: <http://dx.doi.org/10.1063/1.4762832>

View Table of Contents: <http://scitation.aip.org/content/aip/journal/apl/101/17?ver=pdfcov>

Published by the [AIP Publishing](#)



Re-register for Table of Content Alerts

Create a profile.



Sign up today!



Tunable phononic crystals based on cylindrical Hertzian contact

Feng Li,¹ Duc Ngo,² Jinkyu Yang,^{1,a)} and Chiara Daraio³

¹Mechanical Engineering Department, University of South Carolina, 300 Main Street, Columbia, South Carolina 29208, USA

²School of Engineering and Technology, Eastern International University, Binh Duong, Vietnam

³Graduate Aerospace Laboratories (GALCIT), California Institute of Technology, 1200 E. California Blvd., Pasadena, California 91125, USA

(Received 10 August 2012; accepted 9 October 2012; published online 23 October 2012)

We investigate the tunability of phononic crystals consisting of arrays of cylindrical elements using theoretical, numerical, and experimental approaches. We show that when these systems are excited by a continuous dynamic signal under large static precompression, they support a characteristic band structure whose cutoff frequency can be controlled by changing the alignment angles or the static precompression. Furthermore, we report the formation of an additional pass band when there exists particles' eccentricity, which is caused by the coupling mechanism between longitudinal and shear modes. © 2012 American Institute of Physics. [<http://dx.doi.org/10.1063/1.4762832>]

Wave propagation in periodic structures (or phononic crystals, PC) has been extensively studied in the recent years to understand the formation and control of forbidden frequency bands called band gaps. Researchers have shown that the band gaps of PCs composed of elements embedded in host media depend on the characteristics of their materials and configurations, such as geometry,¹ filling fraction,² and stiffness.³ Changes in these characteristics, for example, by manipulation of their structural compositions² or by the application of external fields,⁴ allow for direct modification of the band structure. Recently, granular crystals—a type of nonlinear periodic structure composed of ordered elastic granules—have attracted significant attention due to their versatile mechanical responses stemming from nonlinear Hertzian contact.⁵ Granular crystals under applied static precompression were shown to present band gaps that could be tuned by changing the particles mechanical properties and dimension, as well as the system's static loading.^{6,7} While various configurations of granular crystals have been investigated, most research focused on the dynamic response of systems composed of spherical particles.

In this letter, we describe the responses of one-dimensional granular crystals composed of short cylinders aligned with different relative alignment angles and eccentricities. This study is motivated by the recent finding that the wave propagation in uncompressed chains of cylindrical particles is strongly affected by the alignment angle.⁸ We show that, in a linearized dynamic regime under the effect of large static precompression, the cutoff frequencies of the granular crystals can be tuned over a remarkably wide dynamic range by changing alignment angles and the static precompression applied. Furthermore, we report that an additional pass band at higher frequencies emerges when the cylindrical particles are aligned eccentrically with respect to each other. This band is caused by the transverse movement of the particles. All of these control parameters provide efficient means to manipulate the granular crystals' band

structure, enabling the design of efficient mechanical filters or vibration isolators.

The setup of the experimental system is shown in Fig. 1(a). The cylindrical particles are arranged in an alternating fashion at various alignment angles α , with $\alpha = 0^\circ, 30^\circ, 45^\circ, 60^\circ,$ and 90° , supported by angled L-shaped holders [Fig. 1(b)]. The chain is composed of 16 fused quartz cylinders with radius $R = 18.0$ mm and height $H = 18.0$ mm. A digital photo of the chain is shown in Fig. 1(c). The density $\rho = 2187$ kg/m³, the Young's modulus $E = 72$ GPa, and the Poisson ratio $\nu = 0.17$. The normal compressive force F_0 is applied using a movable rigid block (acting as a wall) on rollers. The amount of static precompression applied is varied at nine different levels ($F_0 = [7.04, 14.08, 21.12, 28.17, 35.21, 42.25, 49.29, 56.33, 63.37]$ N) for each of the corresponding angle of orientation between cylinders.

To investigate the dynamic response of the chain of cylindrical particles, we employ a network analyzer with an electric amplifier, which is connected to a force sensor and a piezoelectric actuator to measure the transfer gain of the system [Fig. 1(a)]. A piezoelectric actuator excites the chain in the axial direction, and a force sensor mounted on the other side of the chain measures the waves propagating through

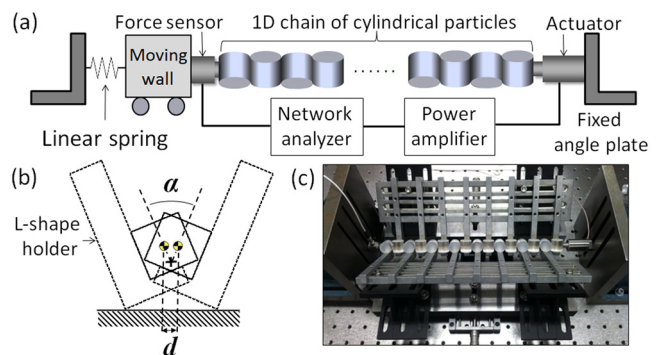


FIG. 1. (a) Schematic of experimental setup composed of a one-dimensional chain of alternating cylindrical particles under precompression. (b) Cross-sectional view of the cylindrical chain with L-shaped holders. (c) Photo of experimental setup.

^{a)}Author to whom correspondence should be addressed. Electronic mail: jkyang@cec.sc.edu.

the chain. The maximum magnitude of the dynamic forces is measured to be 1.78 N, which is approximately an order-of-magnitude smaller than the static precompression.

A chain of cylindrical particles can be modeled as an array of rigid masses connected by nonlinear springs representing the Hertzian contact between particles.⁵⁻⁹ Mathematically, the nonlinear interactions between two adjacent cylindrical particles can be expressed as $F = k_{cyl}\delta^{3/2}$ for $\alpha \neq 0^\circ$, where F and δ are contact force and displacement, respectively.⁸ The contact stiffness k_{cyl} can be expressed as

$$k_{cyl} = \frac{2E}{3(1-\nu^2)} \sqrt{\frac{R}{\sin\alpha}} \left[\frac{2K(e)}{\pi} \right]^{-3/2} \times \left\{ \frac{4}{\pi e^2} \sqrt{\left[\left(\frac{a}{b} \right)^2 E(e) - K(e) \right] [K(e) - E(e)]} \right\}^{1/2}. \quad (1)$$

Here, $E(e)$ and $K(e)$ are the complete elliptic integrals of the first and second kinds, $e = \sqrt{1 - (b/a)^2}$ is the eccentricity of the elliptical contact area between two cylindrical particles, and the ratio between the semi-major axis a and semi-minor axis b is approximated as $b/a \approx [(1 + \cos\alpha)/(1 - \cos\alpha)]^{-2/3}$. It should be noted that the nonlinear interactions in chains of cylinders and spheres are both proportional to the displacement δ to the power $3/2$ in compression. The only difference is that the contact stiffness k_{cyl} exhibits the strong dependence on the alignment angle α , while the contact stiffness between spherical particles does not depend on their transverse arrangements due to the symmetry of the particle's geometry.⁸ For the case $\alpha = 0^\circ$, two adjacent cylinders are in line contact, and the relationship between displacement and contact force in this case does not follow power law exactly as reported in Ref. 8.

The equation of motion for each particle in the chain is given as

$$m\ddot{u}_i = k_{cyl}[\delta_0 + u_{i-1} - u_i]_+^{3/2} - k_{cyl}[\delta_0 + u_i - u_{i+1}]_+^{3/2}. \quad (2)$$

Here, u_i is the displacement of the i th cylindrical particle, $[x]_+$ denotes the positive part of x , and δ_0 is the static displacement caused by precompression F_0 . Under strong precompression ($\delta_0 \gg |u_i - u_{i-1}|$), we can linearize Eq. (2) into

$$m\ddot{u}_i \cong \frac{3k_{cyl}\delta_0^{1/2}}{2} [u_{i-1} - 2u_i + u_{i+1}]. \quad (3)$$

We employ Floquet's theory to relate the dynamics of a particle to that of its neighboring particles based on the periodicity of the system.¹⁰ Mathematically, the particles' displacements can be expressed as $u_{n+1} = u_n e^{-i(4\pi R/\lambda)}$, where λ is the wavelength of the propagating elastic waves. After imposing this theory and the condition of non-trivial solution, we obtain the characteristic equation defining the dispersion relation

$$m\omega^2 = 3k_{cyl}\delta_0^{1/2} [1 - \cos(4\pi R/\lambda)], \quad (4)$$

where ω is the angular velocity of the propagating harmonic waves. This in turn enables the calculations of the cutoff frequency of the chain's pass-band as

$$f_c = \frac{1}{\pi} \sqrt{\frac{3k_{cyl}^{2/3}}{2m}} F_0^{1/6}. \quad (5)$$

The frequency response of a cylindrical chain with alignment angle $\alpha = 60^\circ$ is illustrated in Fig. 2. Given the amount of precompression $F_0 = 28.17$ N, the cutoff frequency is expected to be at 11.74 kHz according to Eq. (5). The numerical simulations using the linearized model⁶ indicate that this cutoff frequency corresponds to the highest resonant mode of the discrete granular chain as shown in Fig. 2(a). This resonant mode represents out-of-phase oscillations of cylindrical particles in the 1D granular chain. The highest resonant frequency ($f_{c,exp}$) measured experimentally is 11.58 kHz, which agrees well with the theoretical value [Fig. 2(b)].

The numerical and experimental results of the normalized power spectral density (PSD) over a range of applied precompression are depicted in Figs. 2(c) and 2(d) respectively. The tunable nature of the cylindrical chain is evident in this figure, which shows that as the applied precompression is gradually increased, the pass-band widens, enabling the transfer of higher frequencies. For example, when the chain is further compressed to the highest compression level ($F_0 = 63.37$ N), the cutoff frequency increases to 13.44 kHz, which is 44.2% larger than the frequency at the lowest precompression ($F_0 = 7.04$ N). We also observe that tunability of the granular chain in terms of the amount of cutoff frequency shift is gradually diminished as a stronger precompression is imposed on the chain.

Figure 3 depicts the cutoff frequencies as a function of precompression for various alignment angles between cylinders. It shows that cutoff frequencies are proportional to $F_0^{1/6}$ [see Eq. (5)]. We observe that the cutoff frequencies can be efficiently tuned by manipulating alignment angles. As the alignment angles between the cylinders are reduced from the 90° to smaller angles, we find the cutoff frequencies increase. For example, under $F_0 = 63.37$ N ($F_0^{1/6} = 2.00$ N^{1/6}), the analytical cutoff frequencies are increased from 13.02 to 15.31 kHz as the alignment angle changes from 90° to 30° .

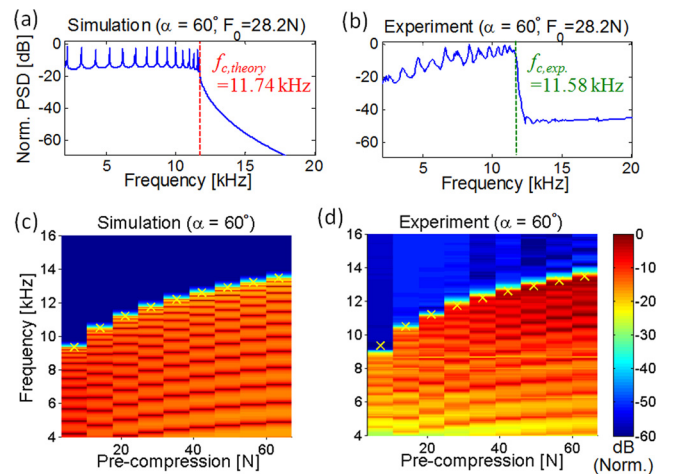


FIG. 2. (a) Numerical and experimental results of normalized transfer gains as a function of frequency for a cylindrical chain with $\alpha = 60^\circ$ and $F_0 = 28.2$ N. (b) Surface maps of numerical and experimental transfer gains as a function of precompression ($\alpha = 60^\circ$). Cross marks represent theoretical cutoff frequencies.

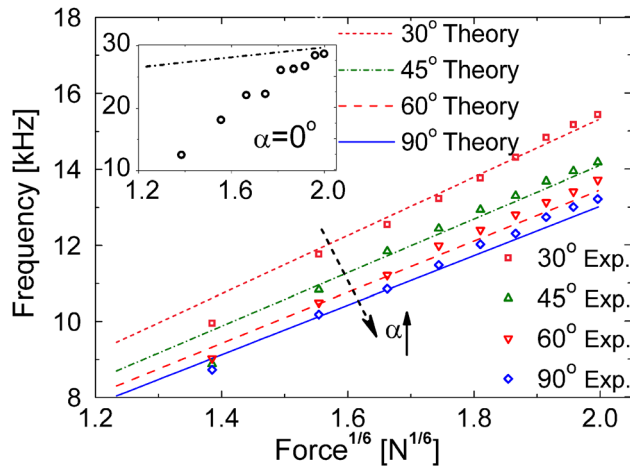


FIG. 3. Theoretical (lines) and experimental (points) values corresponding to the cutoff frequency of chains with different alignment angles between particles. The inset shows the cutoff frequencies for $\alpha = 0^\circ$.

This is due to the increase of the eccentricity (e) of the elliptic contact area from a circle ($e = 0$) to a more elongated ellipse ($e \rightarrow 1$), resulting in increased contact stiffness between particles given the identical precompression. It is also noteworthy that the cutoff frequencies increase dramatically as the alignment angle approaches 0° . This is because the contact area rapidly approximates a line contact as the alignment angle approaches 0° . The cutoff frequency at $F_0 = 63.37$ N is 29.73 kHz, which is almost twice of the cutoff frequency at $\alpha = 30^\circ$. The experimental results corroborate the analytical predictions. However, when the alignment angles are small such as $\alpha = 0^\circ$ or 30° , we find that experimental results tend to underestimate the theoretical cutoff frequencies [inset in Fig. 3]. Such discrepancies can be attributed to the imperfect interface over an elongated contact area caused by the disagreement between the true and nominal contact areas, especially for the case of line contact ($\alpha = 0^\circ$). Such discrepancy is more obvious under the small precompression. In addition, the theoretical contact relationship as expressed in Eq. (1) has its own limitations at small angles, causing noticeable deviations between the predicted cutoff frequencies and the experimental data.^{8,11}

To analyze the effects of the particles' alignment along the chain's axis, we impose eccentricity by varying the particles' offset from 0 to 12 mm [d in Fig. 1(b)]. We find that, in the presence of such offset, an additional pass band emerges at higher frequency ranges. Numerical simulations of the eccentric chains are carried out using 3D finite element analysis (FEA). Figure 4(a) shows the particles' excitation mode when the offset of the chain approaches 0° . In this case, the higher mode is mainly shear (S mode) and cannot be detected by the transducers. As a consequence, in experiments we observe only a single pass-band, whose cutoff frequency corresponds to the upper boundary of the longitudinal mode (L mode). As the offset increases, the S mode couples with the L mode and the particles gradually go into a rotational mode (R mode) [Fig. 4(b)], which can be measured by the compressive force transducer.

The dependence of the experimental cutoff frequencies on the particles' offset is represented in Fig. 4(c). When the offset d increases, a second band appears and becomes wider.

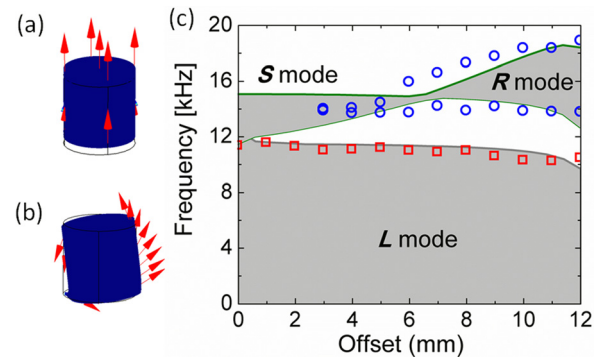


FIG. 4. (a) Finite element results showing the longitudinal modes of the particles when the chain's offset is zero. The arrows indicate the displacements of vibrational modes. In this case, the upper pass-band is in S mode. (b) Finite element results showing the particles' rotational mode when the offset is 12 mm. In this case, the upper pass-band is in R mode. (c) Comparison of the numerical and experimental cutoff frequencies as a function of the chain's offset. The experimental longitudinal modes are indicated by square (red) markers, and the appearance of a second experimental pass-band related to shear modes is indicated by circular (blue) markers.

When $d \neq 0$, the cylinders are no longer symmetric with respect to the wave propagation direction and each cylinder cannot be modeled simply as a lumped mass. In this case, the eccentricity can effectively create a band gap, similar to the band structure formed in a diatomic chain, i.e., a chain composed of periodic unit-cell consisting of two distinct particles.

In conclusion, we assembled chains of identical cylindrical particles oriented at a variable angle with respect to each other and studied the dynamic response of these chains excited by a continuous vibratory signal. We analyzed the effect of static precompression, alignment angles, and particles' eccentricity on the signal's transmissibility. We used theory and numerical simulations to calculate the systems' band structure and compared the results with experiments. We found that the dynamic response of chains of cylindrical particles is highly tunable by variations of the system's alignment angles and precompression. This tunability is particularly evident when the particles are arranged parallel or near parallel with respect to each other. Finally, we demonstrated that, when the centers of mass of the particles are misaligned with respect to the chain's axis, rotational modes can be generated. The rotational modes introduce an additional pass band located above the cutoff frequency of the transmission band. Compared to the classical chains of spherical particles, the granular crystals composed of cylindrical elements provide an added degree of freedom to control the shape and position of frequency band structures by changing their alignment angles and eccentricity levels. The tunability of chains of cylindrical particles obtained with purely mechanical techniques can open an efficient way to create phononic band-gap structures with enhanced controllability that could be used as passive, tunable acoustic filtering devices and vibration absorbers.

¹A. Khelif, P. A. Deymier, B. Djafari-Rouhani, J. O. Vasseur, and L. Dobrzynski, *J. Appl. Phys.* **94**(3), 1308 (2003).

²S.-C. S. Lin and T. J. Huang, *Phys. Rev. B* **83**(17), 174303 (2011).

³L. Jun, W. Yihui, L. Feng, Z. Ping, L. Yongshun, and W. Junfeng, *Europhys. Lett.* **98**(3), 36001 (2012).

- ⁴J. F. Robillard, O. B. Matar, J. O. Vasseur, P. A. Deymier, M. Stippinger, A. C. Hladky-Hennion, Y. Pennec, and B. Djafari-Rouhani, *Appl. Phys. Lett.* **95**(12), 124104 (2009).
- ⁵V. F. Nesterenko, *Dynamics of Heterogeneous Materials* (Springer-Verlag New York, Inc., New York, 2001).
- ⁶N. Boechler, J. Yang, G. Theocharis, P. G. Kevrekidis, and C. Daraio, *J. Appl. Phys.* **109**(7), 074906 (2011).
- ⁷E. Herbold, J. Kim, V. Nesterenko, S. Wang, and C. Daraio, *Acta Mech.* **205**(1), 85 (2009).
- ⁸D. Khatri, D. Ngo, and C. Daraio, *Granular Matter* **14**, 63 (2012).
- ⁹C. Coste, E. Falcon, and S. Fauve, *Phys. Rev. E* **56**(5), 6104 (1997).
- ¹⁰L. Brillouin, *Wave Propagation in Periodic Structures* (Dover, New York, 1953).
- ¹¹K. L. Johnson, *Contact Mechanics* (Cambridge University Press, 1985).